

# Validation of recently released GOCE-based satellite-only global geopotential models over the Red Sea using shipborne gravity data

A. ZAKI<sup>1,2</sup>, A.H. MANSI<sup>3,4</sup>, M. RABAH<sup>5</sup> and G. EL-FIKY<sup>1,6</sup>

<sup>1</sup> Construction Engineering and Utilities Department, University of Zaqazig, Egypt

<sup>2</sup> Department of Civil Engineering, Higher Institute of Engineering in El-Shorouk City, Cairo, Egypt

<sup>3</sup> Istituto Nazionale di Geofisica e Vulcanologia, Sezione di Pisa, Italy

<sup>4</sup> Department of Civil and Environmental Engineering, Politecnico di Milano, Italy

<sup>5</sup> Department of Civil Engineering, University of Benha, Egypt

<sup>6</sup> Higher Institute of Engineering, Belbeis, Egypt

(Received: 5 March 2018; accepted: 31 July 2018)

**ABSTRACT** The gravity field and steady-state ocean circulation explorer (GOCE) satellite, successfully concluded its mission in October 2013 after collecting unprecedented gravity gradient measurements. Such GOCE data made it possible to improve the determination of the geoid over the Red Sea region. The performance of GOCE-based satellite-only global geopotential models (GGMs), at the end of its mission, is evaluated via spectral analysis and by using shipborne free-air gravity anomalies collected over the study area, namely the Red Sea. Eight of the most recent GOCE-based satellite-only GGMs, namely the DIR\_R5, ITU\_GGC16\_2, SPW\_R5, TIM\_R5, NULP\_02S, IfE\_GOCE05s, IGGT\_R1, and GGM05G, are validated. Firstly, the spectral analysis of these GGMs was performed. The DIR\_R5 model showed a superior behaviour, in all terms, in comparison to all the investigated GGMs. Then, the GGMs were evaluated, from spherical harmonics degree/order (d/o) ranging from 100 to their maximum d/o, with respect to the shipborne gravity data after applying the spectral enhancement method, to overcome the existing spectral gap. All the studied GGMs closely calculated the full power of gravity anomaly at a spherical harmonic d/o equivalent to 160. Regardless of the cross-comparable results obtained by the DIR\_R5, TIM\_R5, SPW\_R5, ITU\_GGC16\_2, and IfE\_GOCE05s, whose standard deviation (STD) values of the differences with respect to shipborne data range from 9.90 and 9.93 mGal, the SPW\_R5 model produced the best results with discrepancies characterised with a minimum, maximum, mean, and STD of -56.26, 131.29, 2.07, and 9.90 mGal, respectively.

**Key words:** GOCE, shipborne gravity, Red Sea, satellite-only Global Geopotential Models.

## 1. Introduction

The Red Sea is one of the most important semi-closed waterbodies and its current circulation is one of the most unexplored research field in the northern hemisphere (Rasul *et al.*, 2015).

The gravity field and steady-state ocean circulation explorer (GOCE) mission, launched in orbit on March 2009 and lasting 42 months, successfully collected leading gravity gradient measurements until October 2013 (Bingham *et al.*, 2011). As indicated by its name, the main objective of the GOCE is the determination of the ocean circulation. GOCE provided the scientific community with an unprecedented gravity field for the Earth, in terms of accuracy, more than ever (Haines *et al.*, 2011), so its estimates of the geostrophic currents, in turn, can improve those currents obtained with other satellite missions.

However, semi-enclosed seas, like the Red Sea, are a real challenge for GOCE, since the spatial scales of their structures are, generally, smaller than in the open ocean as well as also being smaller than the expected resolution of GOCE models. Therefore, the study of the geostrophic currents of the Red Sea is considerably complicated and necessitates the availability of a precise geoid with extremely high-resolution and accuracy. The determination of such a high-resolution geoid for marine regions requires integrating heterogeneous gravity data sets provided by different data platforms, e.g. global geopotential models (GGMs), satellite altimetry, and shipborne gravimetric observations, for instance. For more details, the interested reader can consult Kirby and Forsberg (1998); Hwang *et al.* (2002); Novák *et al.* (2003); Hirt *et al.* (2010); Zaki (2015); Braitenberg *et al.* (2016); El-Ashqer *et al.* (2016, 2017); Sampietro *et al.* (2016, 2018a, 2018b); Mansi *et al.* (2018) and Sobh *et al.* (2018).

With regards to the Red Sea, Zaki *et al.* (2018) filtered the shipborne gravity data, provided by the Bureau Gravimétrique International (BGI) (where no metadata were made available on the accuracy of the observations), and used it to assess the performance of the recent releases of various GGMs, i.e. satellite-only and combined models as well as satellite altimetry data. The EGM2008 showed the best results with differences characterised with a mean value of 1.35 mGal ( $1 \text{ mGal} = 1.0 \times 10^{-5} \text{ m} \times \text{s}^{-2}$ ) and a standard deviation (STD) of 11.11 mGal [after applying the spectral enhancement method (SEM)]. However, the EGM2008 is affected by several biases mainly due to datum inconsistencies and variability of the input observations density and accuracy (Pavlis *et al.*, 2008, 2012). The GOCE-based satellite-only GGMs, apart from being more accurate in the medium frequencies (where the effects of the biases in the EGM2008 are bigger), are not affected by local biases since they were developed using globally homogeneous data referred to a unique geocentric ellipsoid: the effects of different data sources and inconsistent height data are therefore absent.

Hence, the challenge is to improve the EGM2008 model by exploiting satellite-only GGMs, specifically based on GOCE data. The quality and performance of the GGMs do not vary only depending on the spatial location of the Earth but also on the different bands of the spectral expansion. Therefore, the spectral validation and the assessment of the GGMs using in-situ data are essential to improve their performances over the study area. Moreover, both the spectral evaluation and the quality assessment of GGMs in each band of the spherical harmonic (SH) expansion spectrum are crucial to gain a clear idea on their commission error contents and consequently to determine the optimal integration SH degree/order (d/o), where the best results are revealed. For such reasons, this study aims to perform an assessment for GOCE-based satellite-only GGMs in the terms of both the spectral assessment using the EGM2008, as a reference model, and the external validation exploiting the shipborne gravity data acquired over the Red Sea.

This research is organized as follows. The theory of the spectral analysis and external validation

are presented in section 2. A brief description of the investigated GGMs is made in section 3. The results of the spectral analysis and the validation with respect to the shipborne gravity data are given in section 4. Finally, some relevant conclusions are drawn in section 5.

## 2. Theoretical background

The GGMs are normally validated using two main approaches. The first is the so-called “internal validation”, which means performing a spectral validation of the GGMs signal and its errors in the form of the degree and error variances. The second refers to the external validation of the GGMs, exploiting external data such as terrestrial gravity and GPS/levelling data at various GGM SH expansions. In the first approach, the absolute sense is done by comparing the behaviour of the model’s SH coefficients over the entire spectral band in terms of degree variances, error degree variances, signal-to-noise ratio (SNR), and cumulative errors per degree. On the other hand, the relative internal validation is implemented to perform a comparison of the spectral behaviour of the studied GGMs with respect to a state-of-the-art GGM, e.g. the EGM2008 in our study. The relative sense is suitable to obtain more detailed insights about the model’s spectral characteristics.

### 2.1. Spectral validation

However, the absolute spectral validation of a GGM can be done using the degree variances, error degree variances, and SNR of the investigated model, which can be directly derived using both the fully normalized potential cosine and sine coefficients ( $\bar{C}_{nm}$  and  $\bar{S}_{nm}$ ) and their error variances  $\sigma_{\bar{C}_{nm}}^2$  and  $\sigma_{\bar{S}_{nm}}^2$ . The degree variances express the power spectrum of the coefficients in each degree or up to a specific degree, if computed cumulatively, as reported in Rapp (1982, 1986):

$$\sigma_n^2 = \sum_{m=0}^n (\bar{C}_{nm}^2 + \bar{S}_{nm}^2). \quad (1)$$

On the other hand, the error degree variances estimate the total error power at a given degree or up to a specific degree, if computed cumulatively, as reported in Eq. 2:

$$\hat{\sigma}_n^2 = \sum_{m=0}^n (\sigma_{\bar{C}_{nm}}^2 + \sigma_{\bar{S}_{nm}}^2) \quad (2)$$

The degree variances and error degree variances can also be computed for any potential functional, such as the gravity anomalies,  $\Delta g$ , by a simple multiplication with the proper eigenvalue in order to obtain the designated functional. Such eigenvalues are summarized in the Meissl’s scheme (Table 1) that provides the spectral linkage between the different functionals of the disturbing potential at different altitudes on the Earth’s surface (Rummel and van Gelderen, 1995). Moreover, the SNR that provides useful information about the relative signal strength given the signal error at a certain degree, can be simply computed as follows:

$$SNR_n = \frac{\sigma_n}{\hat{\sigma}_n} \quad (3)$$

Table 1 - The eigenvalues for some potential functionals according to the Meissl's scheme (Rummel and van Gelderen, 1995).

Potential function	Eigenvalues	Unit
Signal	1	Dimensionless
Disturbing potential ( $T$ )	$\frac{GM}{R}$	$m^2 s^{-2}$
Geoid height ( $N$ )	R	$m$
Gravity anomaly ( $\Delta g$ )	$\frac{GM}{R^2} (n - 1) 10^5$	mGal
Gravity disturbance ( $\Delta g$ )	$\frac{GM}{R^2} (n + 1) 10^5$	mGal
Vertical deflection ( $\theta$ )	$180 \cdot 3600 / \pi$	degree sec

In contrast, the spectral validation in its relative sense is often accomplished by comparing the spectral behaviour of the considered GGMs with a state-of-the-art model, e.g. the EGM2008, in terms of the differences between the degree variances and Gain. The former can be directly achieved by evaluating the differences between the  $\bar{C}_{nm}$  and  $\bar{S}_{nm}$  coefficients of the studied GGM and the reference one as:

$$\Delta \bar{C}_{nm} = \bar{C}_{nm}^{GOCE\_Model} - \bar{C}_{nm}^{EGM2008} \tag{4}$$

$$\Delta \bar{S}_{nm} = \bar{S}_{nm}^{GOCE\_Model} - \bar{S}_{nm}^{EGM2008}$$

By placing  $\Delta \bar{C}_{nm}$ ,  $\Delta \bar{S}_{nm}$  in Eq. 1, it is possible to evaluate the differences of the degree variances between the two models per degree. Additionally, the relative comparison of the formal error magnitudes can be done using the Gain (Sneeuw, 2000), which provides an indicative measure of the improvement achieved by the GOCE GGMs with respect to the reference model. The Gain is expressed as the ratio between the error spectrum of a GGM and the reference model:

$$g_n = \frac{\hat{\sigma}_n^{EGM2008}}{\hat{\sigma}_n^{GOCE\_Model}} \tag{5}$$

### 2.2. External validation

The external validation aims to validate the GGMs with reliable external data of high quality, such as gravity anomaly and GPS-levelling, acquired at different geographic locations. The main problem in comparing satellite-only GGMs with terrestrial data is their different spectral contents. In general, GGMs are limited by their maximum SH d/o, where an omission error is always presented, neglecting the high-degree spectral content. On the other hand, the terrestrial data, in theory, encompasses the full spectra. Different methods have been implemented to overcome such spectral inconsistency in order to achieve an acceptable comparability level between both data typologies, e.g. the low-pass filtering (LPF) and the SEM. The LPF that adopts several techniques, e.g. the spectral or Gaussian filters or least-squares collocation (LSC), may perform well when the terrestrial data are available in some suitable arrangements, for instance, grids, profiles, or at

densely scattered locations (Ihde *et al.*, 2010). However, performing the LPF is a delicate task in the case of very irregularly or scarcely distributed stations, if possible at all. In contrast, the SEM can be used to evaluate GGMs independently of the spatial distribution of the terrestrial data (Hirt *et al.*, 2011). This is the most important advantage when using irregularly distributed ground observations as is often the case with shipborne gravity data, consequently, the SEM will be implemented in this study.

In the SEM, plotted in Fig. 1, the spectral gap between GGMs and terrestrial data is partially overcome by sewing together the high-degree spectral bands of the EGM2008 (Pavlis *et al.*, 2008, 2012) and the omission error estimates sourced from a residual terrain model (RTM) (Forsberg, 1984), which delivers information on the very short wavelengths gravity field constituents (Hirt *et al.*, 2011). Each model of the GOCE-based GGMs under evaluation is expanded to d/o  $n_1$  (e.g. 250), with the EGM2008 used to recover the spectral band starting from  $n_1+1$  (e.g. 251) to  $n_2$  (e.g. 2,190). Beyond d/o  $n_2$ , the RTM omission error estimates are exploited to complete the spectral content of the model as best as possible. The RTM computes the higher frequencies of the gravity field due to the topography/bathymetry as simple as the differences between a detailed digital elevation model (DEM) and a reference topographic one such as the DTM2006.0 (Pavlis *et al.*, 2007) in order to remove a large part of the ‘topographic signals’ already implied by the EGM2008. The RTM gravity signal, in a planar approximation environment, can be computed using the following formula:

$$\delta g = G \iint_E \int_{h_{ref}}^h \frac{\rho(x,y,z)(h_p-z)}{[(x_p-x)^2+(y_p-y)^2+(h_p-z)^2]^{\frac{3}{2}}} dx dy dz \tag{6}$$

where  $E$  is the planar projection of the integration area,  $h_{ref}$  represents the height of the smoothed DEM, i.e. the DTM2006.0 model,  $h$  is the height of the detailed DEM,  $x, y$ , and  $z$  are the Cartesian coordinates of the integrated topographic voxel,  $\rho(x, y, z)$  is the mean reference crustal density of the Earth, i.e.  $2.67 \text{ g}_m \cdot \text{cm}^{-3}$ , and  $x_p, y_p$ , and  $h_p$  are the are the planar coordinates and the height of the computational point in the Cartesian coordinates system, in which the RTM is evaluated on.

The residuals of the processed shipborne gravimetric data are computed by:

$$\Delta g_{res} = \Delta g_{shipborne} - \Delta g_{GOCE\_Model_2}^n - \Delta g_{EGM2008_{n+1}^{2190}} - \Delta g_{RTM} \tag{7}$$

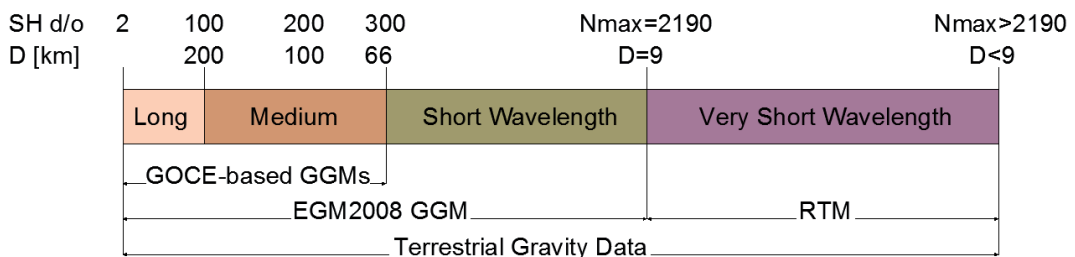


Fig. 1 - The spectral enhancement method (SEM) principle (Zaki *et al.*, 2018).

### 3. GOCE-based satellite-only global geopotential models

In this study, the validation of eight recent releases of GOCE-based satellite-only GGMs, made public by the International Centre for Global Earth Models (ICGEM, GFZ Potsdam), is done by performing the spectral analysis exploiting the shipborne gravity data acquired over the Red Sea. The selected GGMs are carefully selected to represent the various computational approaches used in global gravity field determination.

Some of the GOCE-based satellite-only GGMs are computed using the GRACE mission or combined models as a priori information, therefore we have not only included the so-called GOCE-only models but also the GOCE-combined GGMs that combine GOCE data with other satellite missions. The European Space Agency (ESA) releases GOCE-based GGMs based on three processing algorithms, namely the direct approach, the time-wise approach, and the space-wise approach. For our validation, the latest releases of the fifth generation of the different processing techniques are used, where a summarized review is given in the sequel.

The GOCE-DIR-R5 model (Bruinsma *et al.*, 2014), namely the GO\_CONS\_GCF\_2\_DIR\_R5, available up to d/o 300, was computed by combining the measurements of GOCE gradiometry (full mission), SLR LAGEOS (25 years from 1985 to 2010) to compute the very-low degrees, i.e. 2 and 3, and GRACE normal equation up to d/o 175 (10 years from 2003 to 2012). Afterwards, while combining GRACE with GOCE, the contributions of the former were considered only up to d/o 130. During the processing phase of the GOCE gravity gradients, the *a priori* considered gravity field was obtained from the GOCE-model fourth release, GO\_CONS\_GCF\_2\_DIR\_R4, computed using the direct approach up to its maximum d/o 260. In addition, a regularization spherical cap (Metzler and Pail, 2005) was iteratively computed up to d/o 300 and a Kaula regularization was applied to all coefficients beyond d/o 180.

The GOCE-TIM-R5 model (Pail *et al.*, 2011), namely the GO\_CONS\_GCF\_2\_TIM\_R5, available up to SH d/o 280, was computed using the least-squares adjustment of the full GOCE satellite gravity gradiometry (SGG) measurements and satellite-to-satellite tracking (SST) data. The SST part of the normal equations was estimated up to d/o 150 using the short-arc integral approach (Mayer-Gürr *et al.*, 2005) applied to the GOCE kinematic orbits, while the SGG part was estimated up to the maximum solvable d/o. Furthermore, a Kaula regularization was applied to the near-zonal coefficients in order to overcome the polar gap problem and to coefficients of d/o 201 to 280 to enhance the SNR.

The GOCE-SPW-R5 model (Gatti *et al.*, 2016), namely the GO\_CONS\_GCF\_2\_SPW\_R5, produced to a maximum d/o of 330, was directly evaluated by SH analysis of GOCE observations, which have been previously gridded at satellite altitude using global LSC. The fifth generation of the space-wise model has been computed from the SGG and SST observations of the full GOCE mission using no prior information.

The GGM05G model (Bettadpur *et al.*, 2015) of a maximum d/o of 240, was calculated from the GOCE SGG data collected for the entire mission using a bandpass filter of 10-50 MHz, filling the polar gap with synthetic gradients from the GGM05S model (Tapley *et al.*, 2013) up to d/o 150 evaluated at a 200 km altitude, GRACE K-band intersatellite range-rate data, GPS tracking, and GRACE accelerometer data. The GGM05G is not regularized in any way, where the errors increase with the increase of d/o. It is not recommended to use the GGM05G beyond approximately d/o 210 without accounting for some smoothing (Bettadpur *et al.*, 2015).



The ITU\_GGC16\_2 model (Akyilmaz *et al.*, 2016) of a maximum d/o of 280 was developed combining the normal equations of the ITU\_GRACE16\_2 (up to d/o 180) and the GO\_CONS\_GCF\_2\_TIM\_R5 (up to d/o 280) (Brockmann *et al.*, 2014). The combination was performed at the normal equation level with the optimal variance component estimation.

The NULP-02s model (Marchenko *et al.*, 2017) is available at a maximum d/o of 250, based on the radial derivatives of the entire GOCE mission and the radial derivatives of the EGM2008 up to d/o 360 to overcome the polar gaps and its instability. Consequently, its related error coefficients are not provided, therefore for the calculations that depend on the formal errors, this model will not be considered.

The IfE\_GOCE05s model (Wu *et al.*, 2016), which is a GOCE-only GGM developed by the Institut für Erdmessung (IfE), Leibniz Universität Hannover Germany, is available up to a maximum d/o of 250 and was computed using only the entire GOCE observations, i.e. orbit and gravity gradients. The acceleration approach was applied to the kinematic orbit data in order to derive the model up to d/o 150. The GOCE SGG data were then used to complete the model to its maximum d/o. A slight Kaula-regularization was applied to improve the SNR of the coefficients between d/o 201 and 250.

The IGGT\_R1 model (Lu *et al.*, 2018) of a maximum d/o of 240 has used the GOCE SGG data to create the gravitational gradient normal equation from d/o 2 to 150. For d/o 150 and higher, the Kaula's rule is applied to the normal equation because for this degree range the low-order coefficients as well as all other short wavelength SH coefficients are disturbed by the polar gap and the increasing sensitivity of the GOCE gradiometer.

In summary, a total of eight recently GOCE-based satellite-only GGMs have been used as reported in Table 2.

Table 2 - The main properties and characteristics of the GOCE-based satellite-only GGMs used in this study.

Model	Max degree	GOCE [month]	GRACE [year]	LAGEOS-SLR [year]	Year of release
DIR_R5	300	~42	10	25	2014
TIM_R5	280	~42	-	-	2014
SPW_R5	330	~42	-	-	2017
GGM05G	240	~42	5	-	2015
ITU_GGC16_2	280	~42	10	-	2017
NULP_02S	250	~42	-	-	2017
IfE_GOCE05s	250	~42	-	-	2017
IGGT_R1	240	~13	-	-	2017

#### 4. Results

This part reports the results of the executed spectral analysis, as well as the validation, performed using the shipborne gravity.

4.1. Spectral validation

The absolute spectral analysis of the square root of the degree variances and error degree variances related to the gravity anomalies for all GOCE-based GGMs are plotted in Fig. 2a. Special attention will be given to d/o 200, which coincides with the aspired GOCE spatial resolution of 100

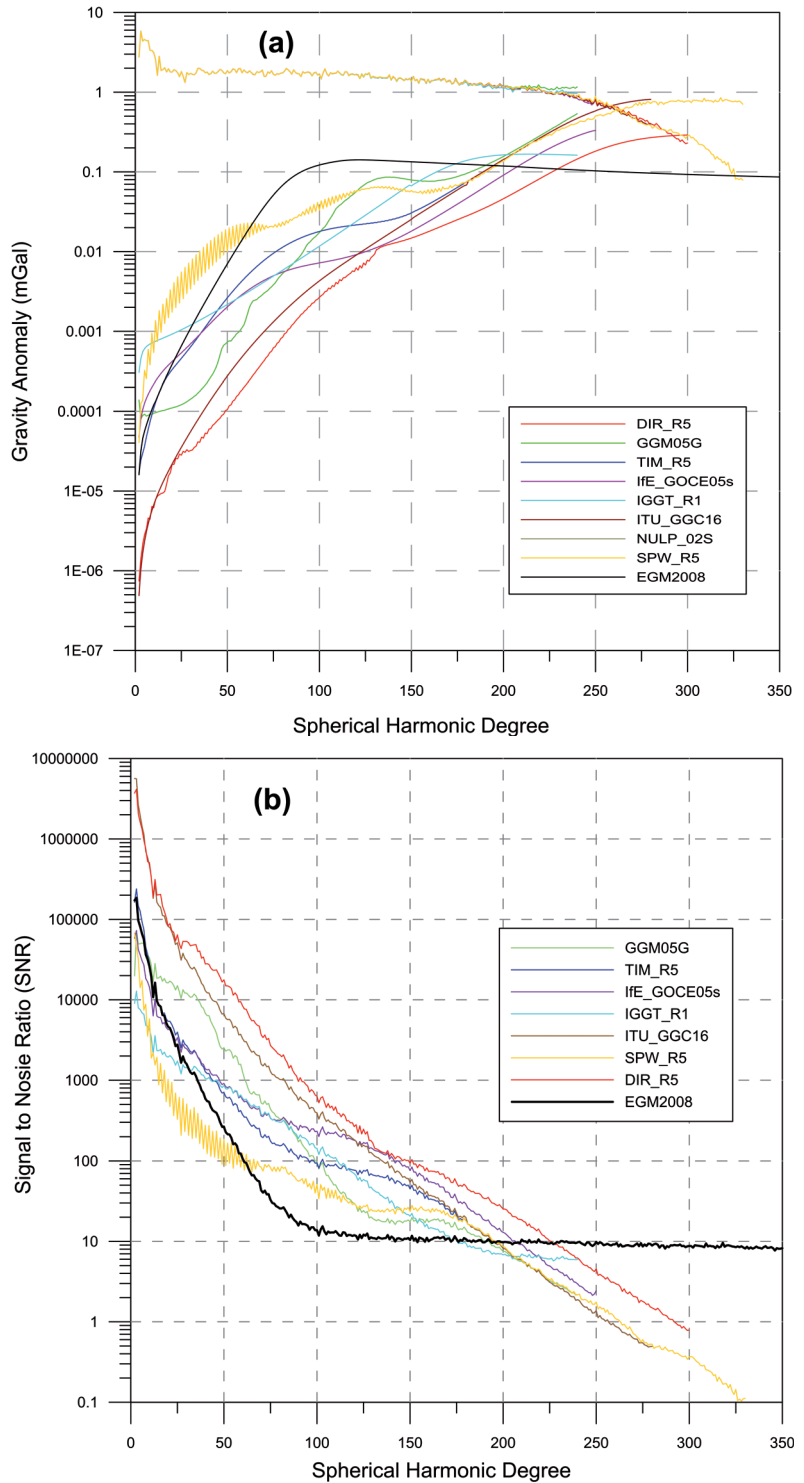


Fig. 2 - The square root of degree variances and the error degree variances related to the gravity anomalies of GOCE GGMs (a) and the SNR for GOCE models (b).



km. The various investigated GGMs did not show any visible differences in the degree variance up to d/o 200. The DIR\_R5 model displays a superior behaviour in terms of formal errors with respect to the other models and its provided error spectrum is below that of the EGM2008 up to d/o 230. The DIR\_R5 shows smaller errors for the long-wavelengths due to the inclusion of both the GRACE and LAGEOS data to elaborate and produce the long-wave potential coefficients. In the meanwhile, the ITU\_GGC16\_2 gave the second smaller formal errors up to d/o 130 due to the use of the ITU\_GRACE16\_2 as a prior gravity field. The IfE\_GOCE05s gave the second smaller formal errors beyond d/o 130. The compatibility between the ITU\_GRACE16\_2 and the TIM\_R5 beyond d/o 180 is justifiable as the TIM\_R5 was used to determine the ITU\_GRACE16\_2 beyond d/o 180 (Akyilmaz *et al.*, 2016). Fig. 2b depicts the SNR for the evaluated GGMs. As can be clearly seen, the DIR\_R5 retains a better performance compared to the EGM2008 over the entire spectrum up to d/o 227, while the IfE\_GOCE05s has a better performance compared to the EGM2008 up to d/o 208. The SNR of the SPW\_R5 is worse than the EGM2008 up to d/o 60 and better from d/o 61 to 195. At d/o 200 (spatial resolution of 100 km), the DIR\_R5 is the best model with a SNR equivalent to 25 followed by the IfE\_GOCE05s that illustrated a SNR of 12.78 at the same d/o.

In terms of the cumulative gravity anomalies errors, shown in Fig. 3, the DIR\_R5 showed the overall best error spectrum with the smallest cumulative gravity errors at all the investigated d/o, thereby emphasizing the benefits of using the combined satellite-only (GOCE and GRACE) GGMs. The DIR\_R5 reaches the 1.0 mGal error at d/o 258, the IfE\_GOCE05s at d/o 231, while the IGGT\_R1 model is the worst GGM, in which the same error was achieved at a lower d/o of 204. At d/o 200, minimum cumulative errors of 0.21 and 0.36 mGal were computed for the DIR\_R5 and the IfE\_GOCE05s, respectively. Beyond d/o 290, the EGM2008 shows the smallest cumulative errors in comparison to the other models.

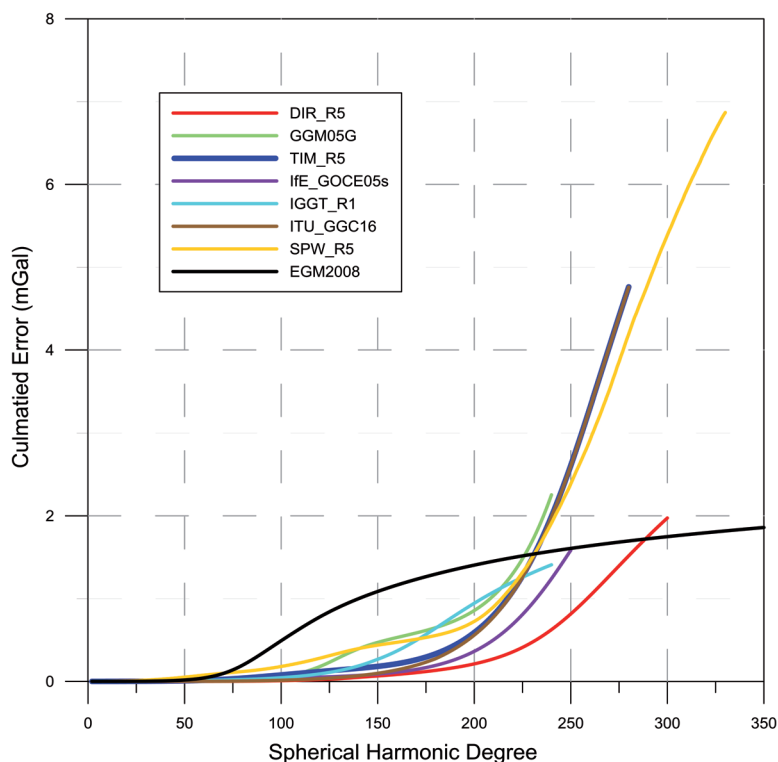


Fig. 3 - The cumulative errors of GOCE GGMs and the EGM2008 in terms of gravity anomalies.

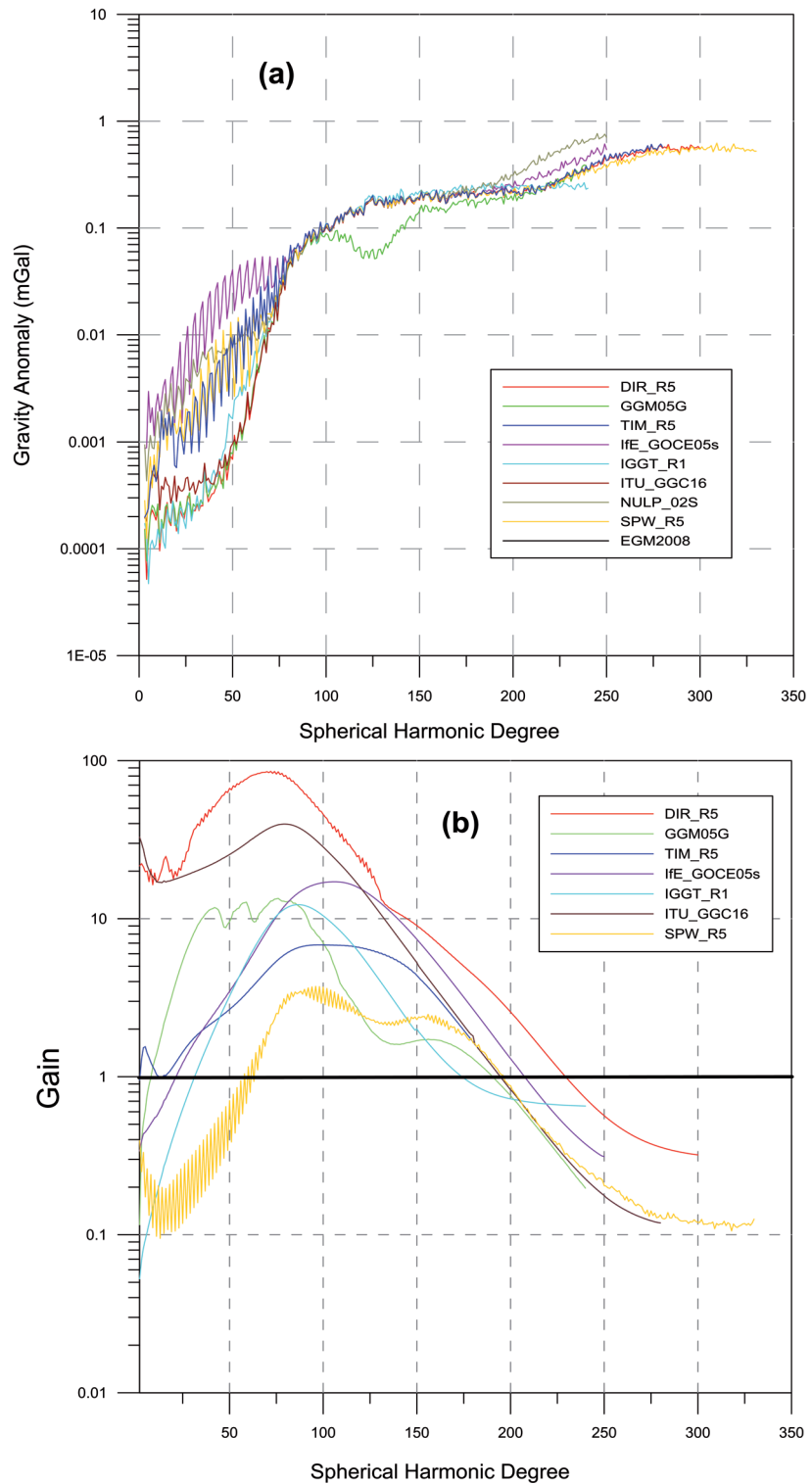


Fig. 4 - A visual representation for the obtained results: a) the difference of the degree variances in terms of gravity anomalies between the GOCE-based GGMs and the EGM2008. Unit = mGal; b) the Gain of GOCE-based GGMs with respect to the EGM2008.

By studying Fig. 4a, that visualises the differences of the degree variances in terms of gravity anomalies between the GOCE-based GGMs and the EGM2008, some points can be addressed. On one hand, the DIR\_R5 outperformed the IfE\_GOCE05s as well as the TIM\_R5, in particular at

the long-wavelengths of the gravitational spectrum, where the observations of GRACE and LAGEOS are exploited for the development of the DIR\_R5 solutions, as mentioned earlier. The IfE\_GOCE05s showed the highest differences at lower degrees. The reason for such a behaviour could be the fact that for the development of this model neither a reference model nor any prior gravity information were considered.

On the other hand, Fig. 4b displays the Gain of the GOCE GGMs with respect to the EGM2008. The useful spectral band offered by the latest GOCE-based satellite-only models becomes apparent in terms of significant digits of the model Gain compared to the EGM2008. This band ranges between d/o 60 and 197 for the SPW\_R5, up to d/o 195 for the ITU\_GGC16\_2, and d/o 230 for the DIR\_R5.

**4.2. Validation with the shipborne gravity data**

A total number of 95,649 shipborne gravity stations were provided by the BGI along with their spatial distribution as reported in Fig. 5. A rigorous data filtering has been applied to the shipborne data set using the approach described in Zaki *et al.* (2018) based on the leave-one-out cross-validation technique (Arlot and Celisse, 2010) and the Kriging prediction algorithm (Matheron, 1963). The leave-one-out process, with a strict confidence level of 95.4%, is repeatedly applied until the STD of the residuals, i.e. the difference between the observed and interpolated values, is smaller than 1.5 mGal. The shipborne free-air (FA) gravity anomalies are characterised by a minimum, maximum, mean, and STD of -202.15, 113.50, -20.17, and 34.05 mGal, respectively.

The comparison between the GGMs and the EGM2008 with the shipborne gravity data before applying the SEM is shown in Table 3. All GOCE-based models were outperformed by the EGM2008 due to the spectral gaps between satellite-only GGMs and the terrestrial (i.e. marine) gravity data, where the SPW\_R5 showed the best results with a mean value of -13.04 mGal and an STD of 33.19 mGal.

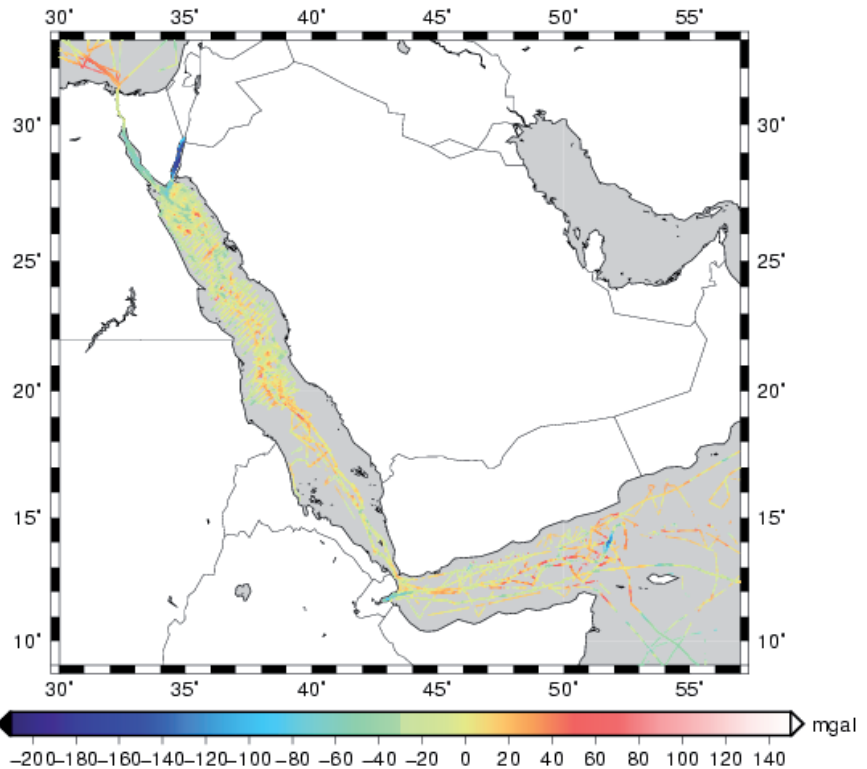


Fig. 5 - The spatial distribution and FA gravity anomalies of the 95649 shipborne stations (Zaki *et al.*, 2018).

Table 3 - The statistics of the differences between the GOCE-based GGMs and the shipborne gravity data (95,649 stations) before applying the SEM. Unit = mGal.

Model	Degree	Minimum	Maximum	Mean	STD
DIR_R5	300	-216.72	123.59	-13.44	35.68
TIM_R5	280	-196.40	121.47	-12.74	33.69
SPW_R5	330	-196.81	120.77	-13.04	<b>33.19</b>
GGM05G	240	-201.85	125.30	-12.83	34.23
ITU_GGC16_2	280	-196.45	121.54	-12.75	33.69
NULP_02S	250	-215.75	128.91	-13.88	36.25
IfE_GOCE05s	250	-215.65	127.5	-14.21	35.74
IGGT_R1	240	-189.82	120.46	-10.32	34.73
EGM2008	2190	-55.57	136.22	-0.50	11.27

The SEM has been implemented to fill in the existing spectral gap between the studied GGMs and the shipborne gravity data by combining the high-degree bands of the EGM2008 with the very high-frequency signal delivered by the RTM (Forsberg, 1984), which has been proven to improve the performance of several GGMs in medium-elevated and rugged terrain (Forsberg, 1985; Hirt *et al.*, 2010; Sampietro *et al.*, 2017; Capponi *et al.*, 2018). The RTM signal, which is computed as the difference between the terrain effects, resulted from the 15 arc-second shuttle radar topography mission (SRTM) (USGS, 2017), i.e. the SRTM15+ model, and the reference surface resulted by smoothing such detailed digital terrain model using the TC Grid (Forsberg and Tscherning, 2008) routine of the GRAVSOFT package, in a 5×5 arc-minute grid in order to remove a large part of the ‘spectral information’ already implied by the EGM2008. Although the DTM2006.0 (Pavlis *et al.*, 2007) was considered, it was not used in this study because it has lower resolution and less

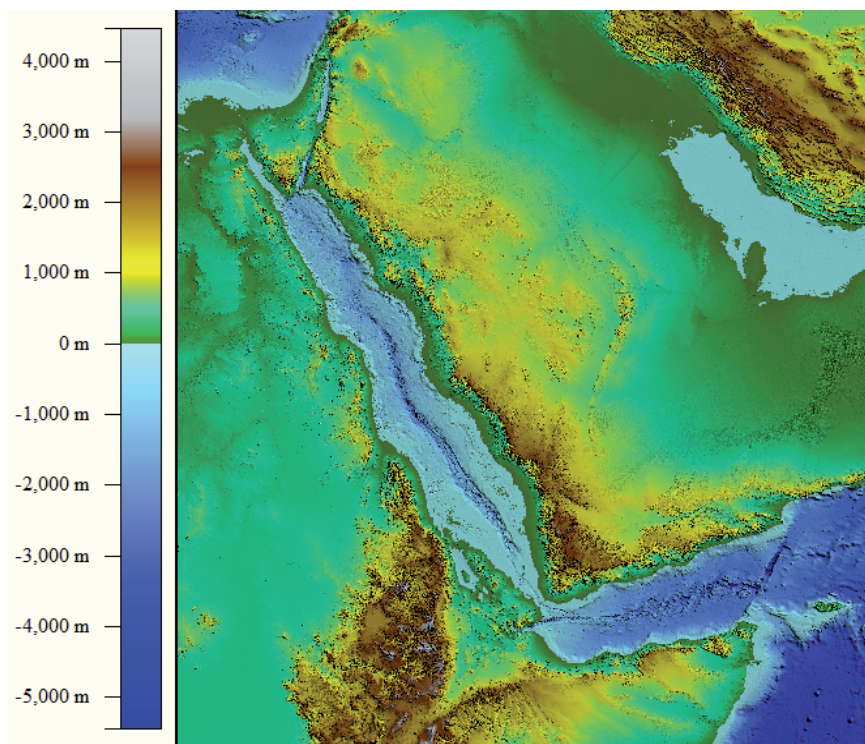


Fig. 6 - The SRTM 15+ model for Red Sea region. Unit = m.

information content about the bathymetry in the Red Sea compared to the SRTM15+ (Fig. 6). The RTM has been computed utilising the TC toolbox of the GRAVSOFT package (Forsberg and Tscherning, 2008) with an integration radius of 100 km and with the standard crustal density value of 2.67 g/cm<sup>3</sup>. The residuals of the processed shipborne gravimetric data are computed using Eq. 7.

Table 4 and Fig. 7 report the statistics of the differences of the various GGMs and the shipborne gravity data after applying the SEM from d/o 100 to the maximum d/o of the investigated models

Table 4 - The statistics of the differences between the GOCE-based GGMs and the shipborne gravity data (95,649 stations) after applying the SEM. Unit = mGal.

<b>DIR_R5</b>	<b>100</b>	<b>120</b>	<b>140</b>	<b>160</b>	<b>180</b>	<b>200</b>	<b>220</b>	<b>240</b>	<b>260</b>	<b>280</b>	<b>300</b>		
Minimum	-54.53	-55.00	-57.97	-56.10	-58.31	-54.30	-52.60	-53.34	-56.42	-68.55	-68.17		
Maximum	130.51	130.82	131.00	131.62	131.50	131.63	130.59	132.96	130.87	130.79	129.41		
Mean	2.05	2.97	3.12	2.14	1.41	1.03	0.37	-0.48	0.01	-0.17	-0.53		
STD	10.17	10.17	10.19	<u>9.92</u>	10.26	10.35	10.64	11.62	11.72	12.19	12.83		
<b>TIM_R5</b>	<b>100</b>	<b>120</b>	<b>140</b>	<b>160</b>	<b>180</b>	<b>200</b>	<b>220</b>	<b>240</b>	<b>260</b>	<b>280</b>	<b>300</b>		
Minimum	-54.57	-55.16	-58.30	-56.28	-58.56	-54.08	-52.01	-51.68	-54.42	-67.20			
Maximum	130.47	130.80	130.86	131.45	131.11	131.55	131.12	134.87	135.24	135.18			
Mean	2.04	3.00	3.08	2.12	1.32	0.90	0.31	-0.35	0.16	-0.11			
STD	10.17	10.20	10.19	<u>9.92</u>	10.28	10.38	10.73	11.58	11.57	11.90			
<b>SPW_R5</b>	<b>100</b>	<b>120</b>	<b>140</b>	<b>160</b>	<b>180</b>	<b>200</b>	<b>220</b>	<b>240</b>	<b>260</b>	<b>280</b>	<b>300</b>	<b>320</b>	<b>330</b>
Minimum	-54.52	-55.15	-58.28	-56.26	-58.63	-54.55	-53.03	-56.95	-58.96	-72.69	-73.55	-78.55	-79.55
Maximum	130.52	130.90	130.99	131.29	130.96	131.29	126.42	125.78	123.90	125.69	121.46	120.16	119.46
Mean	2.07	3.03	3.10	2.07	1.40	0.98	0.01	-0.31	0.17	-0.01	-0.17	-0.22	-0.18
STD	10.18	10.20	10.19	<u>9.90</u>	10.31	10.40	10.99	11.23	11.61	12.07	12.19	12.46	12.96
<b>GGM05G</b>	<b>100</b>	<b>120</b>	<b>140</b>	<b>160</b>	<b>180</b>	<b>200</b>	<b>220</b>	<b>240</b>	<b>260</b>	<b>280</b>	<b>300</b>		
Minimum	-54.41	-54.47	-55.79	-54.85	-56.23	-52.63	-48.74	-47.18					
Maximum	130.22	130.22	130.69	130.91	131.04	131.72	131.17	130.30					
Mean	2.05	2.64	2.81	2.53	2.04	1.58	0.99	0.07					
STD	10.17	10.16	10.13	<u>10.07</u>	10.39	10.42	10.68	11.60					
<b>ITU_GGC16_2</b>	<b>100</b>	<b>120</b>	<b>140</b>	<b>160</b>	<b>180</b>	<b>200</b>	<b>220</b>	<b>240</b>	<b>260</b>	<b>280</b>	<b>300</b>		
Minimum	-54.54	-55.14	-58.28	-56.30	-58.58	-54.10	-52.03	-51.70	-54.38	-67.21			
Maximum	130.47	130.78	130.88	131.46	131.15	131.59	131.16	134.91	135.28	135.22			
Mean	2.05	2.99	3.08	2.12	1.31	0.90	0.31	-0.36	0.16	-0.12			
STD	10.17	10.19	10.20	<u>9.92</u>	10.29	10.38	10.73	11.58	11.57	11.91			
<b>NULP-02s</b>	<b>100</b>	<b>120</b>	<b>140</b>	<b>160</b>	<b>180</b>	<b>200</b>	<b>220</b>	<b>240</b>	<b>250</b>	<b>280</b>	<b>300</b>		
Minimum	-54.52	-55.42	-58.67	-56.92	-59.28	-55.43	-52.23	-57.50	-66.15				
Maximum	130.85	132.13	130.93	131.00	130.77	132.60	128.94	127.69	125.77				
Mean	2.11	2.85	3.21	1.92	1.16	0.61	-0.32	-0.69	-0.88				
STD	10.19	10.20	10.25	<u>9.91</u>	10.25	10.41	10.88	11.58	11.82				
<b>lfe_GOCE05s</b>	<b>100</b>	<b>120</b>	<b>140</b>	<b>160</b>	<b>180</b>	<b>200</b>	<b>220</b>	<b>240</b>	<b>250</b>	<b>280</b>	<b>300</b>		
Minimum	-55.14	-55.42	-54.41	-56.46	-52.63	-55.43	-54.54	-58.50	-67.15				
Maximum	130.31	131.11	130.93	131.13	130.96	131.35	127.11	124.78	123.93				
Mean	2.08	2.95	3.15	2.14	1.15	0.62	-0.23	-0.75	-0.85				
STD	10.21	10.20	10.13	<u>9.93</u>	10.35	10.38	10.65	11.69	11.64				
<b>IGGT_R1</b>	<b>100</b>	<b>120</b>	<b>140</b>	<b>160</b>	<b>180</b>	<b>200</b>	<b>220</b>	<b>240</b>	<b>250</b>	<b>280</b>	<b>300</b>		
Minimum	-56.52	-55.42	-59.58	-57.38	-56.23	-55.43	-52.23	-57.50					
Maximum	132.31	131.20	132.43	128.52	131.72	132.60	128.94	127.69					
Mean	2.12	2.85	3.11	2.60	1.22	0.62	-0.23	-0.75					
STD	10.22	10.42	10.35	<u>10.31</u>	10.39	10.49	10.92	11.55					

with an incremental step of 20 d/o. All models provided the full power of the gravity anomaly up to SH d/o 160. The IGGT\_R1 showed the worst behaviour with a mean value of 2.60 and an STD of 10.31 mGal, in which the reason may be the use of only 13 months of the GOCE data. The DIR\_R5, TIM\_R5, SPW\_R5, ITU\_GGC16\_2, and IfE\_GOCE05s gave very close and cross-comparable results at d/o 160. The SPW\_R5 showed a slightly better validation characterised with a minimum, maximum, mean, and STD of -56.26, 131.29, 2.07, and 9.90 mGal, respectively. A note must be taken that the results obtained by the various investigated GGMs at d/o 160 delivered semi-identical STD of the differences with shipborne data, whereas the difference between the STD of the best and the worst model, namely the SPW\_R5 (9.90 mGal) and the IGGT\_R1 (10.31 mGal) model, respectively, is 0.41 mGal, which is, in any case, less than the uncertainty of the leave-one-out cross-validation technique equivalent to 1.5 mGal.

In order to further emphasize the differences between the GGMs and shipborne data at both the maximum d/o of the model as well as d/o 160, the histograms of the differences in both cases were plotted.

Fig. 8 displays the histograms of the differences after applying the SEM at the maximum d/o of the investigated GGM, while Fig. 9 shows those in correspondence to d/o 160. The two sets of figures show the improvement of histogram shapes between the maximum d/o and the d/o 160.

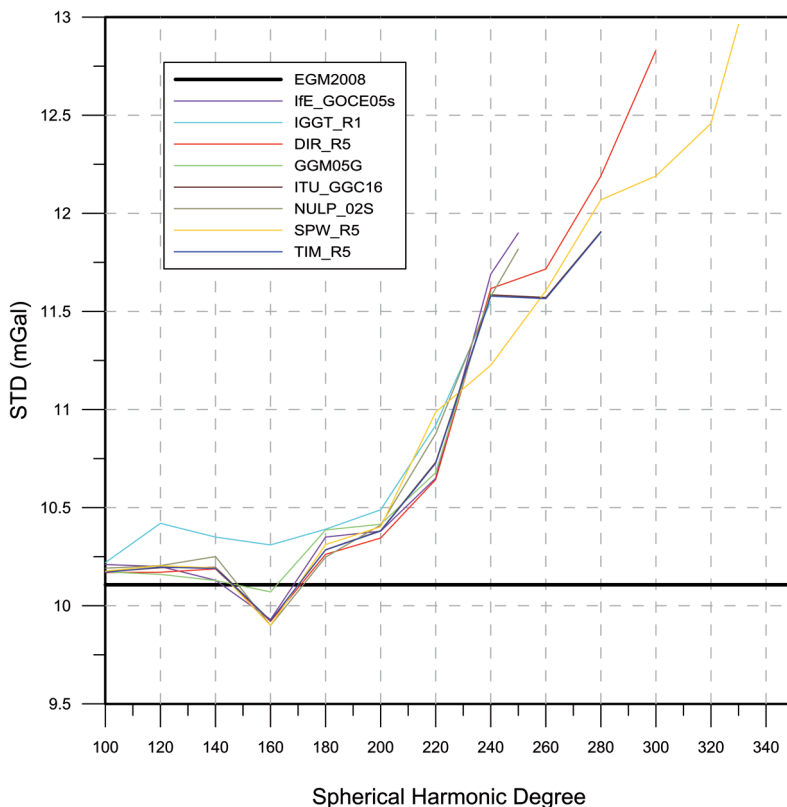


Fig. 7 - A visual representation of the STD of the differences between the GOCE-based GGMs and the shipborne gravity data after applying the SEM (see Table 2). Unit = mGal.



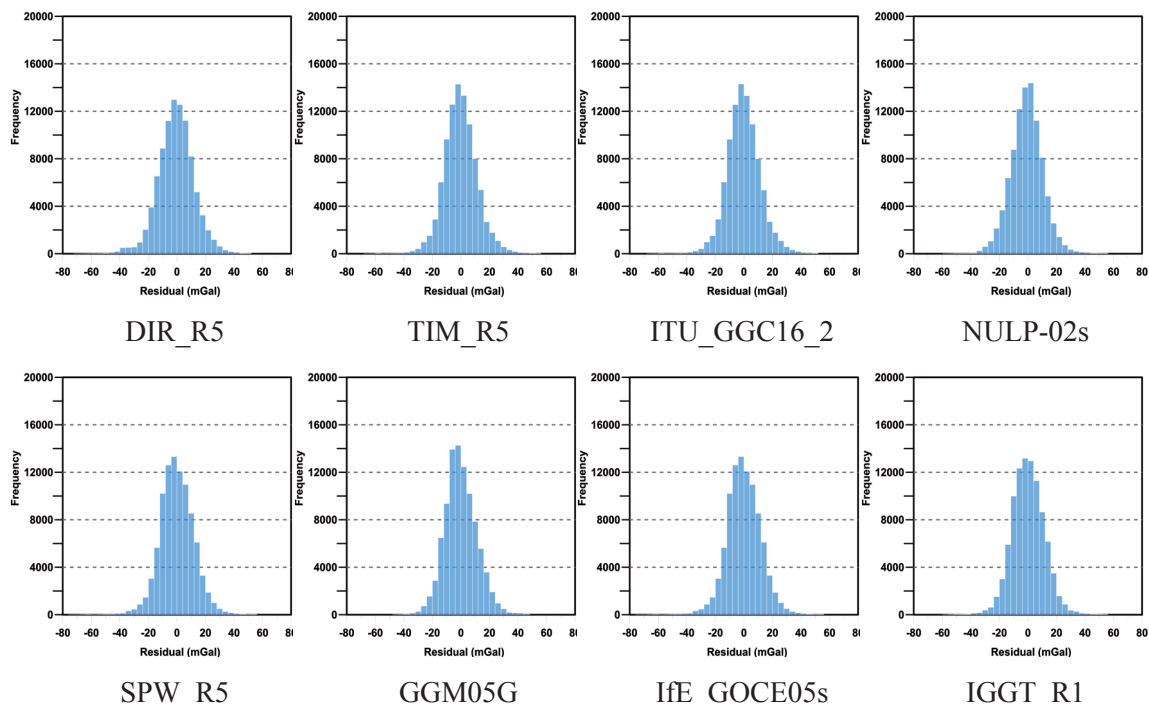


Fig. 8 - The histogram of the differences between GOCE-based GGMs and the shipborne gravity data after applying the SEM at the maximum degree of each model. Unit = mGal.

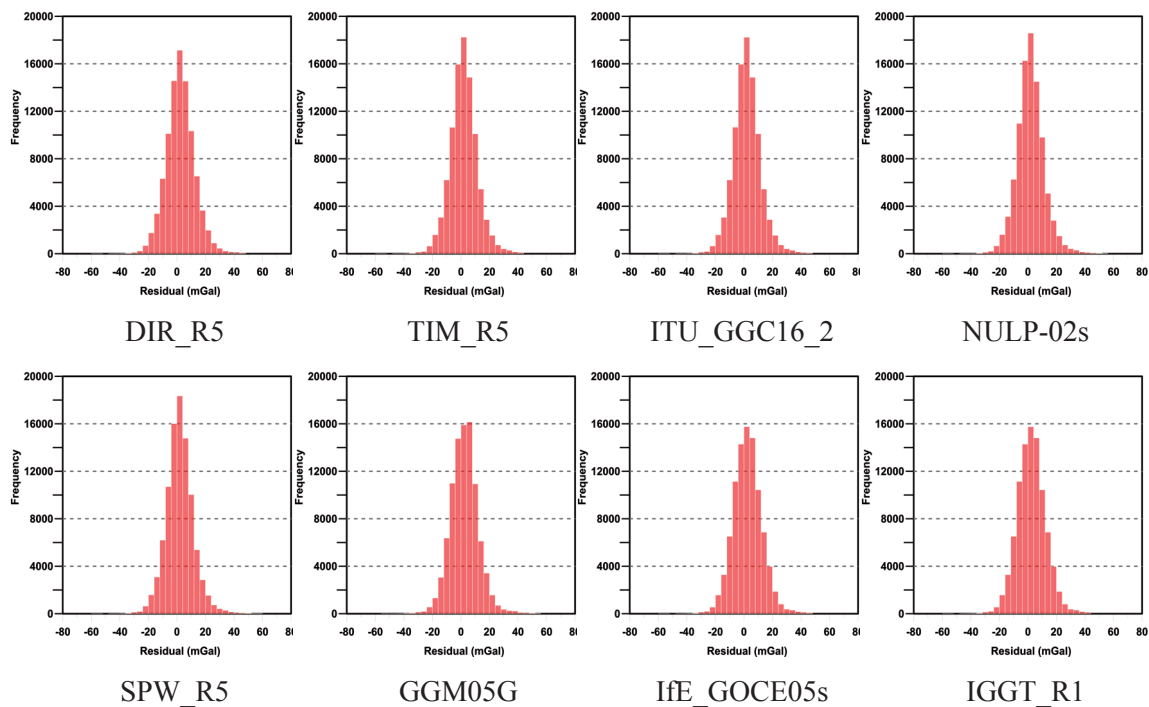


Fig. 9 - The histogram of the differences between the GOCE-based GGMs and the shipborne gravity data after applying the SEM at degree/order 160. Unit = mGal.

## 5. Conclusion

The aim of this study is to validate the recent releases of GOCE-based satellite-only GGMs with the shipborne gravity data acquired over the Red Sea. Firstly, the absolute and relative spectral analyses of eight GGMs, which cover the different processing approaches, i.e. the direct, time-wise, and space-wise approaches, were performed. The DIR\_R5 model showed a superior behaviour with respect to all the investigated models, in all senses and terms. Then, the performance of the various GGMs was evaluated with respect to the shipborne gravity data before and after applying the SEM.

On the one hand, before applying the SEM, all models showed worse results due to the spectral gaps between satellite-only GGMs and the shipborne gravity data. The SPW\_R5 demonstrated the best results, which is characterised by a mean of -13.04 mGal and an STD of 33.19 mGal.

On the other hand, after applying the SEM, all the studied GGMs provided the full power of the gravity anomaly up to SH d/o 160. The DIR\_R5, TIM\_R5, SPW\_R5, ITU\_GGC16\_2, and IfE\_GOCE05s gave very similar results, in which the corresponding STD of the differences ranged from 9.90 and 9.93 mGal. The minimum spectral validation STD was obtained by the SPW\_R5 model, whose differences with respect to the shipborne gravity data are characterised with a minimum, maximum, mean, and STD of -56.26, 131.29, 2.07, and 9.90 mGal, respectively.

In conclusion, due to the superior behaviour obtained, it was the DIR\_R5 model, in all senses, during the spectral validation as well as its semi-identical results to the SPW\_R5 model, which had the best performance when validated with shipborne data. Moreover, due to the similar STD of the differences with the shipborne data of 9.92 and 9.90 mGal, for the DIR\_R5 and SPW\_R5 model, respectively, which is less than the expected uncertainty of the leave-one-out cross-validation technique (equivalent to 1.5 mGal), the DIR\_R5 model is recommended for the integration with the terrestrial data, over the Red Sea, and for its geodetic applications, e.g. the geoid determination and the geostrophic currents estimation.

## References

- Akyilmaz O., Ustun A., Aydın C., Arslan N., Doganalp S., Guney C., Mercan H., Uygur S.O., Uz M. and Yağcı O.; 2016: *High resolution gravity field determination and monitoring of regional mass variations using low-earth orbit satellites*. ICGEM, GFZ Data Services, Potsdam, Germany, Final Report Project 113Y155, 86 pp. (in Turkish).
- Arlot S. and Celisse A.; 2010: *A survey of cross-validation procedures for model selection*. Stat. Surv., **4**, 40-79, doi:10.1214/09-ss054.
- Bettadpur S., Ries J., Eanes R., Nagel P., Pie N., Poole S., Richter T. and Save H.; 2015: *Evaluation of the GGM05 mean earth gravity model*. Geophys. Res. Abstracts, Vienna, Austria, vol. 17, EGU2015-4153.
- Bingham R., Knudsen P., Andersen O. and Pail R.; 2011: *An initial estimate of the North Atlantic steady-state geostrophic circulation from GOCE*. Geophys. Res. Lett., **38**, L01606, doi:10.1029/2010GL045633.
- Braitenberg C., Sampietro D., Pivetta T., Zuliani D., Barbagallo A., Fabris P., Rossi L., Julius F., and Mansi A.H.; 2016: *Gravity for detecting caves: airborne and terrestrial simulations based on a comprehensive karstic cave benchmark*. Pure Appl. Geophys., **173**, 1243-1264, doi:10.1007/s00024-015-1182-y.
- Brockmann J.M., Zehentner N., Höck E., Pail R., Loth I., Mayer-Gürr T. and Schuh W.D.; 2014: *EGM\_TIM\_RL05: an independent geoid with centimeter accuracy purely based on the GOCE mission*. Geophys. Res. Lett., **41**, 8089-8099, doi:10.1002/2014GL061904.
- Bruinsma S.L., Förste C., Abrikosov O., Lemoine J.M., Marty J.C., Mulet S., Rio M.-H. and Bonvalot S.; 2014: *ESA's satellite-only gravity field model via the direct approach based on all GOCE data*. Geophys. Res. Lett., **41**, 7508-7514, doi:10.1002/2014GL062045.
- Capponi M., Mansi A.H. and Sampietro D.; 2018: *Improving the computation of the gravitational terrain effect close to ground stations in the GTE software*. Stud. Geophys. Geod., **62**, 206-222, doi:10.1007/s11200-017-0814-3.

- El-Ashquer M., Elsaka B. and El-Fiky G.; 2016: *On the accuracy assessment of the latest releases of GOCE satellite-based geopotential models with EGM2008 and terrestrial GPS/levelling and gravity data over Egypt*. Int. J. Geosci., **7**, 1323-1344, doi:10.4236/ijg.2016.711097.
- El-Ashquer M., Elsaka B. and El-Fiky G.; 2017: *EGY-HGM2016: an improved hybrid local geoid model for Egypt based on the combination of GOCE-based geopotential model with gravimetric and GNSS/levelling measurements*. Arabian J. Geosci., **10**, 251, doi:10.1007/s12517-017-3042-9.
- Forsberg R.; 1984: *A study of terrain reductions, density anomalies and geophysical inversion methods in gravity field modelling*. Department of Geodetic Science and Surveying, Ohio State University, Columbus, Ohio, OH, USA, Report 355.
- Forsberg R.; 1985: *Gravity field terrain effect computations by FFT*. Bull. Géod., **59**, 342-360, doi:10.1007/BF02521068.
- Forsberg R. and Tscherning C.C.; 2008: *GRAVSOFTE. An overview manual for the GRAVSOFTE geodetic gravity field modelling programs*, 2nd ed. Contract report for JUPEM.
- Gatti A., Reguzzoni M., Migliaccio F. and Sansò F.; 2016: *Computation and assessment of the fifth release of the GOCE-only space-wise solution*. IGFS Meeting, Thessaloniki, Greece, doi:10.13140/RG.2.2.28625.94569.
- Haines K., Johannessen J., Knudsen P., Lea D., Rio M.-H., Bertino L., Davidson F. and Hernandez F.; 2011: *An ocean modelling and assimilation guide to using GOCE geoid products*. Ocean Sci., **7**, 151-164, doi:10.5194/os-7-151-2011.
- Hirt C., Featherstone W. and Marti U.; 2010: *Combining EGM2008 and SRTM/DTM2006. 0 residual terrain model data to improve quasigeoid computations in mountainous areas devoid of gravity data*. J. Geod., **84**, 557-567, doi:10.1007/s00190-010-0395-1.
- Hirt C., Gruber T. and Featherstone W.; 2011: *Evaluation of the first GOCE static gravity field models using terrestrial gravity, vertical deflections and EGM2008 quasigeoid heights*. J. Geod., **85**, 723-740, doi:10.1007/s00190-011-0482-y.
- Hwang C., Hsu H. and Jang R.; 2002: *Global mean sea surface and marine gravity anomaly from multi-satellite altimetry: applications of deflection-geoid and inverse Vening Meinesz formulae*. J. Geod., **76**, 407-418, doi:10.1007/s00190-002-0265-6.
- Ilde J., Wilmes H., Müller J., Denker H., Voigt C. and Hosse M.; 2010: *Validation of satellite gravity field models by regional terrestrial data sets*. In: Flechtner F., Gruber T., Guentner A., Manda M., Rothacher M., Schoene, T. and Wickert J. (eds), System Earth via Geodetic-Geophysical Space Techniques, Springer-Verlag Berlin-Heidelberg, Germany, pp. 277-296, doi:10.1007/978-3-642-10228-8\_22.
- Kirby J. and Forsberg R.; 1998: *A comparison of techniques for the integration of satellite altimeter and surface gravity data for geoid determination*. In: Forsberg R., Feissel M. and Dietrich R. (eds), Geodesy on the Move, International Association of Geodesy Symposia, Springer-Verlag, Berlin-Heidelberg, Germany, vol. 119, pp. 207-212, doi:10.1007/978-3-642-72245-5\_29.
- Lu B., Luo Z., Zhong B., Zhou H., Flechtner F., Förste C., Barthelmes F. and Zhou R.; 2018: *The gravity field model IGGT\_R1 based on the second invariant of the GOCE gravitational gradient tensor*. J. Geod., **92**, 561-572, doi:10.1007/s00190-017-1089-8.
- Mansi A.H., Capponi M. and Sampietro D.; 2018: *Downward continuation of airborne gravity data by means of the change of boundary approach*. Pure Appl. Geophys., **175**, 977-988, doi:10.1007/s00024-017-1717-5.
- Marchenko A.N., Marchenko D.A. and Lopushansky A.N.; 2017: *Gravity field models derived from the second degree radial derivatives of the GOCE mission: a case study*. Ann. Geophys., **59**, s0649-s0659, doi:10.4401/ag-7049.
- Matheron G.; 1963: *Principles of geostatistics*. Econ. Geol., **58**, 1246-1266, doi:10.2113/gsecongeo.58.8.1246.
- Mayer-Gürr T., Ilk K., Eicker A. and Feuchtinger M.; 2005: *ITG-CHAMP01: a CHAMP gravity field model from short kinematic arcs over a one-year observation period*. J. Geod., **78**, 462-480, doi:10.1007/s00190-004-0413-2.
- Metzler B. and Pail R.; 2005: *GOCE data processing: the spherical cap regularization approach*. Stud. Geophys. Geod., **49**, 441-462, doi:10.1007/s11200-005-0021-5.
- Novák P., Kern M., Schwarz K.P., Sideris M., Heck B., Ferguson S., Hammada Y. and Wei M.; 2003: *On geoid determination from airborne gravity*. J. Geod., **76**, 510-522, doi:10.1007/s00190-002-0284-3.
- Pail R., Bruinsma S., Migliaccio F., Förste C., Goiginger H., Schuh W., Höck E., Reguzzoni M., Brockmann J.M. and Abrikosov O.; 2011: *First GOCE gravity field models derived by three different approaches*. J. Geod., **85**, 845-860, doi:10.1007/s00190-011-0467-x.
- Pavlis N.K., Factor J.K. and Holmes S.A.; 2007: *Terrain-related gravimetric quantities computed for the next EGM*. In: Proc. 1<sup>st</sup> Int. Symp. International Gravity Field Service (IGFS), Istanbul, Turkey, Special Issue 18, pp. 318-323.
- Pavlis N.K., Holmes S.A., Kenyon S.C. and Factor J.K.; 2008: *An earth gravitational model to degree 2160: EGM2008*. In: Proc. of European Geosciences Union, Vienna, Austria.

- Pavlis N.K., Holmes S.A., Kenyon S.C. and Factor J.K.; 2012: *The development and evaluation of the Earth Gravitational Model 2008 (EGM2008)*. J. Geophys. Res., **117**, B04406, doi:10.1029/2011JB008916.
- Rapp R.H.; 1982: *A Fortran program for the computation of gravimetric quantities from high degree spherical harmonic expansions*. Department of Geodetic Science and Surveying, Ohio State University, OH, USA, Report 334.
- Rapp R.H.; 1986: *Global geopotential solutions*. In: *Mathematical and Numerical Techniques in Physical Geodesy*, Lecture Notes in Earth Sciences, Springer-Verlag, Berlin-Heidelberg, Germany, vol. 7, pp. 365-415.
- Rasul N.M., Stewart I.C. and Nawab Z.A.; 2015: *Introduction to the Red Sea: its origin, structure, and environment*. In: Rasul N.M. and Stewart I.C. (eds), *The Red Sea, The formation, morphology, oceanography and environment of a young ocean basin*, Springer-Verlag, Berlin-Heidelberg, Germany, pp. 1-28, doi: 10.1007/978-3-662-45201-1\_1.
- Rummel R. and van Gelderen M.; 1995: *Meissl scheme-spectral characteristics of physical geodesy*. Manuscripta Geod., **20**, 379-385.
- Sampietro D., Capponi M., Triglione D., Mansi A.H., Marchetti P. and Sansò F.; 2016: *GTE: a new software for gravitational terrain effect computation: theory and performances*. Pure Appl. Geophys., **173**, 2435-2453, doi:10.1007/s00024-016-1265-4.
- Sampietro D., Capponi M., Mansi A.H., Gatti A., Marchetti P. and Sansò F.; 2017: *Space-Wise approach for airborne gravity data modelling*. J. Geod., **91**, 535-545, doi:10.1007/s00190-016-0981-y.
- Sampietro D., Mansi A.H. and Capponi M.; 2018a: *A new tool for airborne gravimetry survey simulation*. Geosci., **8**, 292, doi:10.3390/geosciences8080292.
- Sampietro D., Mansi A.H. and Capponi M.; 2018b: *Moho depth and crustal architecture beneath the Levant Basin from global gravity field model*. Geosci., **8**, doi:10.3390/geosciences8060200.
- Sneeuw N.; 2000: *A semi-analytical approach to gravity field analysis from satellite observations*. Ph.D. Thesis in Geodesy, University München, Germany.
- Sobh M., Mansi A.H., Ebbing J. and Campbel S.; 2018: *Regional gravity field model of Egypt based on the satellite and ground-based data*. Pure Appl. Geophys., doi:org/10.1007/s00024-018-1982-y.
- Tapley B., Flechtner F., Bettadpur S. and Watkins M.; 2013: *The status and future prospect for GRACE after the first decade*. In: AGU Fall Meeting Abstracts, San Francisco, CA, USA, Abstract G32A-01
- USGS; 2017: *Shuttle radar topography mission*. <earthexplorer.usgs.gov> (Accessed 2-1-2018).
- Wu H., Müller J. and Brieden P.; 2016: *The IfE global gravity field model from GOCE-only observations*. The International Symposium on Gravity, Geoid and Height Systems, Thessaloniki, Greece.
- Zaki A.; 2015: *Assessment of GOCE Models in Egypt*. Master Thesis of Science in Civil Engineering-Public Works, Cairo University, Giza, Egypt, 116 pp., doi:10.13140/RG.2.1.4357.9045.
- Zaki A., Mansi A.H., Selim M., Rabah M. and El-Fiky G.; 2018: *Comparison of satellite altimetric gravity and global geopotential models with shipborne gravity in the Red Sea*. Mar. Geod., **41**, 258-269, doi:10.1080/01490419.2017.1414088.

**Corresponding author:** Ahmed Hamdi Mansi  
Istituto Nazionale di Geofisica e Vulcanologia, Sezione di Pisa  
Via Uguccione della Faggiola 32, 56126 Pisa, Italy  
Phone: +39 050 8311947; e-mail: ahmed.mansi@ingv.it